SLEEPJ, 2019, 1–10

doi: 10.1093/sleep/zsz053
Advance Access Publication Date: 7 March 2019
Original Article

ORIGINAL ARTICLE

The heritability of the human K-complex: a twin study

Maurizio Gorgoni[1], Flaminia Reda[1], Aurora D'Atri[1], Serena Scarpelli[1], Michele Ferrara[2,] and Luigi De Gennaro[1,*,]

[1]Department of Psychology, University of Rome "Sapienza," Rome, Italy and [2]Department of Biotechnological and Applied Clinical Sciences, University of L'Aquila, L'Aquila, Italy

*Corresponding author. Luigi De Gennaro, University of Rome "Sapienza," Via dei Marsi, 78, 00185 Rome, Italy. Email: luigi.degennaro@uniroma1.it.

Abstract

Sleep electroencephalogram (EEG) has a trait-like nature. Several findings highlighted the heritability of spectral power in specific frequency ranges and sleep spindles during nonrapid eye movement (NREM) sleep. However, a genetic influence on the K-complex (KC), one of the electrophysiological hallmarks of NREM sleep, has never been assessed. Here, we investigated the heritability of the KC detected during NREM stage 2 comparing 10 monozygotic (MZ) and 10 dizygotic (DZ) twin pairs. Genetic variance analysis (GVA) and intraclass correlation coefficients (ICCs) were performed to assess the genetic effect and within-pair similarity for KC density, amplitude, and for the area under the curve (AUC) of the KC average waveform at Fz, Cz, and Pz scalp locations. Moreover, cluster analysis was performed on the KC average waveform profile. We observed a significant genetic effect on KC AUC at Cz and Pz, and on amplitude at Pz. Within-pair similarity (ICCs) was always significant for MZ twins except for KC density at Fz, whereas DZ twins always exhibited ICCs below the significance threshold, with the exception of density at Pz. The largest differences in within-pair similarity between MZ and DZ groups were observed again for AUC at Cz and Pz. MZ pairs accurately clustered for the KC average waveform with a higher frequency (successful clustering rate for MZ pairs: Fz = 60%; Cz = 80%; Pz = 90%) compared with DZ pairs (successful clustering rate for DZ pairs: Fz = 10%; Cz = 10%; Pz = none). Our results suggest the existence of a genetic influence on the human KC, particularly related to its morphology and maximally observable in central and parietal locations.

Statement of Significance

In the present study, we assess for the first time the heritability of the human K-complex (KC), comparing monozygotic and dizygotic twin pairs. We found a genetic influence on the morphological parameters and the peak-to-peak amplitude of the KC. This result strengthens the view that electroencephalogram during NREM sleep represents one of the most heritable traits of the human beings. Moreover, starting from the observation of KCs changes in Alzheimer's disease, our findings underline the role of KCs as a potential biomarker for cognitive deterioration, pointing to the importance of the assessment of KC morphology in normal and pathological conditions.

Key words: K-complex; EEG; sleep; twins; heritability; genetics

Submitted: 31 July, 2018; **Revised:** 16 January, 2019

Introduction

The human sleep electroencephalogram (EEG) exhibits trait-like characteristics. The EEG during nonrapid eye movement (NREM) and rapid eye movement (REM) sleep is characterized by high intraindividual stability across time and, conversely, by high interindividual variability [1–5]. This individual sleep EEG-trait remains stable after experimental manipulations that affect sleep features [6–8]. Trait-like features of the sleep EEG show relative stability also across adolescent development [9], despite the intense maturational changes that characterize the sleep EEG during this period.

Such fingerprint-like aspects of the human sleep EEG may be based on a genetic contribution that can be investigated by comparing monozygotic (MZ) and dizygotic (DZ) twin pairs. Early observations showed that sleep profiles were more similar in MZ than in DZ pairs [10], but the investigations on sleep architecture provided partially inconsistent results [11–14]. Stronger evidence for genetic regulation of the sleep EEG came from the analysis of spectral and microstructural aspects. De Gennaro and coworkers [15] found a higher similarity in MZ compared with DZ pairs in the 8–16 Hz frequency range during NREM sleep, that reached a heritability estimate of 96% not influenced by sleep deprivation, promoting the notion of the sleep EEG profile as one of the most heritable traits in humans. Ambrosius and coworkers [16] found a genetic influence on the human NREM sleep spectral composition in the δ (0.75–4.5 Hz), θ (4.75–7.75 Hz), α (8.0–11.75 Hz), and σ (12.0–15.75 Hz) frequency bands. More recently, the genetic effects on architecture, spectral composition and phasic features of REM sleep have been investigated, showing a genetic influence on all of the assessed EEG frequency bands, on several phasic REM parameters, and the morphology of the EEG frequency spectrum [17]. A genetic contribution has also been individuated for the topographical distribution of the sleep EEG during adolescence [18, 19].

Two EEG hallmarks of NREM sleep, the K-complex (KC) and the sleep spindle, fall in frequency ranges (δ and σ, respectively) that seem to undergo a genetic influence. This observation raises the possibility that such NREM graphoelements may be under genetic control. In fact, as previously observed, a genetic component has been reported for NREM sleep σ activity [15, 16], the typical frequency range of the sleep spindles [20]. Consistently, strong genetic influence on several slow spindle parameters has been recently found [21]. Albeit the observed genetic influence on the δ activity [16, 19], the heritability of the KC has never been investigated.

The KC is an isolated downstate [22], characterized by duration >0.5 s, frequency <1 Hz [23–25], and frontal predominance [26, 27]. It can occur spontaneously, but it can also be elicited by different kinds of stimuli [28, 29]. Both the spontaneous and stimulus-elicited KCs represent the EEG graphoelement with the highest amplitude during normal sleep and mainly consists of a slow and large negative component. When elicited by an external stimulus, the large negative peak occurs at about 550 ms, and a later positive peak at about 900 ms. Several studies point to a cortical origin of the KCs [22, 25, 30, 31] and a thalamic mediation of the cortically generated KCs [25, 32].

There is not a definitive consensus about the functional role of the sleep KCs. On the one hand, it has been considered as associated with arousal-related processes [33, 34]: KCs are similar to evoked potentials [27, 35] and can be elicited by different sensory stimuli [28, 29]. On the other hand, a protective role of the KCs on sleep has been suggested [22, 28, 36–38]: KC density increases prior to transition to slow-wave sleep (SWS) compared with transition to REM sleep [39] and decreases across sleep cycles, parallel with a reduction in NREM sleep depth [40]. Moreover, KCs more likely occur during a recovery night following fragmented sleep [37]. A possible two-sided nature of the KC has been proposed: it may represent at the same time a low-level information processing and a sleep-protecting mechanism [32, 41–44].

Understanding the possible genetic influence on the human KC is relevant in light of the proposed role of KC alteration as a biomarker of cognitive deterioration [45]. In fact, KCs seem to be affected by normal and pathological aging. During normal aging, a reduction of the spontaneous KCs [46, 47] and a decrease in incidence and amplitude of the evoked KCs [48–50] have been observed. As far as pathological aging is concerned, several studies showed that patients affected by Alzheimer's disease (AD) are characterized by alterations of spontaneous and evoked KCs [45, 51–55]. In particular, we recently found a strong reduction (more than 40%) of KC density during stage 2 NREM in people with AD (compared with healthy elderly controls) that was related to the degree of cognitive impairment, allowing a correct classification of 80% [45].

The aim of the present study was to assess for the first time the heritability of the KC with a classical twin study, comparing several KC parameters in MZ and DZ twin pairs.

Materials and Methods

Participants

Data for the present analyses were obtained by the sample of the twin study described in De Gennaro et al. [15]. Forty healthy participants, corresponding to 20 Caucasian twin pairs (10 MZ, mean age ± *SE* = 24.1 ± 1.00 years; 10 DZ, mean age ± *SE* = 23.4 ± 0.87 years), were recruited from a university student population. Five MZ and DZ twin pairs were women. With the aim to reduce as much as possible the environmental contribution, we selected only pairs with same gender.

Zygosity was determined by standardized questionnaire and morphological examination, and confirmed by DNA-based analysis. DNA was extracted from cheek cells collected by means of a sponge-tipped swab. Six highly polymorphic short tandem-repeat loci were used to determine homozygosity. With these markers, the probability that any twin pair was MZ if all markers were concordant was 99.9%.

Further inclusion criteria were normal sleep duration and schedule (habitual sleep time: 12:00 am–8:00 am ± 1 hr); no daytime nap habits; no excessive daytime sleepiness; and no other sleep, medical, or psychiatric disorder, as assessed by a 1 week sleep log and by a clinical interview. With respect to zygosity and sex, the groups were not different in their habitual sleep time (MZ: male pairs = 457.5 ± 11.0 min; female pairs = 453.0 ± 11.4 min; DZ: male pairs = 456.0 ± 8.7 min; female pairs = 432.6 ± 11.1 min) and their habitual caffeine consumption (MZ: male pairs = 2.1 ± 0.7 cups/day; female pairs = 2.8 ± 0.9 cups/day; DZ: male pairs = 2.6 ± 0.5 cups/day; female pairs = 1.5 ± 0.2 cups/day). During the week preceding the study, participants did not take any kind of medication (including contraceptives). Both MZ and DZ twins were reared together. Participants were required

to avoid napping throughout the experiment; compliance was controlled by actigraphic recordings (AMI Ambulatory Monitoring, Inc., Mini motion logger, Ardsley, NY). The study on the female twin pairs has been conducted during the follicular phase of their menstrual cycle.

All participants gave their written informed consent. The study was approved by the local institutional ethics committee and was conducted in accordance with the Declaration of Helsinki.

Procedure

After 2 weeks of regular sleep/wake habits monitored with sleep log and (in the last 2 days before the beginning of the study) actigraphic recordings, participants took part in a sleep/wake protocol across 4 consecutive days and nights. Sleep was recorded in a soundproof, temperature-controlled room during the first night (adaptation), the second night (baseline), and the fourth night (recovery sleep after 36 hr of sleep deprivation). For the present study, only the baseline night was considered.

The participant sleep was undisturbed, started at midnight, and finished after 7.5 hr of total sleep time.

EEG recordings

An Esaote Biomedica VEGA 24 (Esaote Biomedica, Florence, Italy) polygraph was used for polygraphic recordings. EEG signals were analogically filtered (high-pass filter with a time constant of 0.3 s and low-pass filter at 30 Hz). The 19 unipolar EEG derivations of the international 10–20 system were recorded from scalp electrodes with averaged mastoid reference. The submental electromyogram (EMG) was recorded with a time constant of 0.03 s. The bipolar horizontal electrooculogram (EOG) was recorded from electrodes placed approximately 1 cm from the medial and lateral canthi of the dominant eye with a time constant of 1 s. Impedance of these electrodes was kept below 5 kΩ. The polygraphic signals were analog-to-digital converted online with a sampling rate of 128 Hz and stored on the disk of a personal computer.

Details about the sleep macrostructure in the MZ and DZ groups during the considered baseline night are reported in De Gennaro et al. [15]. Here we report only time spent in sleep stage 2 (MZ = 258.2 ± 9.01 min; DZ = 266.5 ± 9.3 min), SWS (MZ = 52.03 ± 6.5 min; DZ = 38.2 ± 5.4 min), and REM sleep (MZ = 104.4 ± 5.9 min; DZ = 107.6 ± 3.4 min): no differences between groups have been observed for these parameters.

KC detection

Spontaneous KCs were visually identified by a single blind scorer (F.R.) during NREM stage 2 sleep at Fz, Cz, and Pz. To score a KC, the following criteria were applied: a nonstationary event with (1) a marked and well-delineated sharp wave initially negative in polarity, followed by a positive polarity component occurring approximately 300–400 ms later, detectable over at least one of the midsagittal derivations; (2) amplitude ≥ 75 μV of the negative component, with a maximum at frontocentral derivations; (3) a minimum duration of 0.5 s and a maximum duration of 3 s. If multiple KCs appeared in sequence, only the first one was considered [45, 56].

For each midline derivation, KC density was calculated as the number of KCs divided by NREM stage 2 sleep minutes. For each KC, the peak-to-peak amplitude was calculated as the difference between the large negative peak characterizing the KC and the following (300–400 ms later) large positive peak. To reduce the possible influence of noise in the peak amplitude measures, the mean of the data points around the maximum positive and minimum values (±25 ms) was considered as the positive and negative peaks, respectively. Then, for each participant, the mean amplitude of the KCs was considered as the individual average peak-to-peak amplitude for subsequent analyses.

To obtain a more accurate measure of the morphology of the KCs, the individual KCs were averaged using the maximum negative peak as point for alignment and considering an interval that goes from 550 ms before to 950 ms after such negative peak, obtaining for each participant the individual KC average waveform with a duration of 1500 ms and a negative peak at 550 ms. Figure 1 depicts the average waveforms in two representative MZ (Figure 1a) and DZ (Figure 1b) twin pairs at Fz, Cz, and Pz for illustrative purposes. The difference (absolute values) between the twins belonging to the same pair in each data point of the individual average waveform is also reported in Figure 1c, showing a larger difference between DZ than MZ twins. The area under the curve (AUC) of the KC average waveform (absolute values) was calculated by the trapezoidal rule (TRAPZ function in MATlab) in the given time range (the entire 1500 ms period considered, from 550 ms before to 950 ms after the negative peak). This method approximates the AUC circumscribing the number of trapezoids under a curve. Then, the areas of the trapezoids are summed to obtain the total AUC.

Statistical Analysis

Genetic variance analysis

For each derivation, we assessed MZ and DZ twins with the aim to separate the variance of each variable (KC density, amplitude, and AUC) into environmental and genetic components [16, 17, 21, 57, 58]. Two independent estimates of genetic variance can be calculated: the within-twin pair estimate (GWT) and the within- plus among-twin pair component estimate (GCT). Although GWT depends only on mean squares (MS) for within-pair variation, GCT depends on MS of both within- and among-twin pair components. The choice of the genetic variance estimate was determined by a test of equality of variances (F′ test) for MZ and DZ twins, with α fixed at 0.2 [17, 21, 57, 58]. When MZ and DZ variances were significantly different, we used the GCT, otherwise we used the GWT test. For each variable, two prerequisites had to be fulfilled: (1) normal distribution in both twin samples, measured by a nonsignificant goodness-of-fit by the Shapiro–Wilk test; (2) equal means between MZ and DZ twin samples, measured by *t*-test. The presence of a significant difference between MZ and DZ twin samples would point to the existence of an association between the assessed variable and the type of twins being studied, biasing the estimation of genetic variance [21]. For this reason, genetic variance analysis (GVA) was not performed if there was evidence for significantly different means between MZ and DZ samples. If the criterion of normal distribution was not fulfilled, data were log-transformed. We used MANCOVA to assess the influence of covariates (age and sex). Prerequisites were considered not fulfilled for a $p < 0.05$ at the specific test.

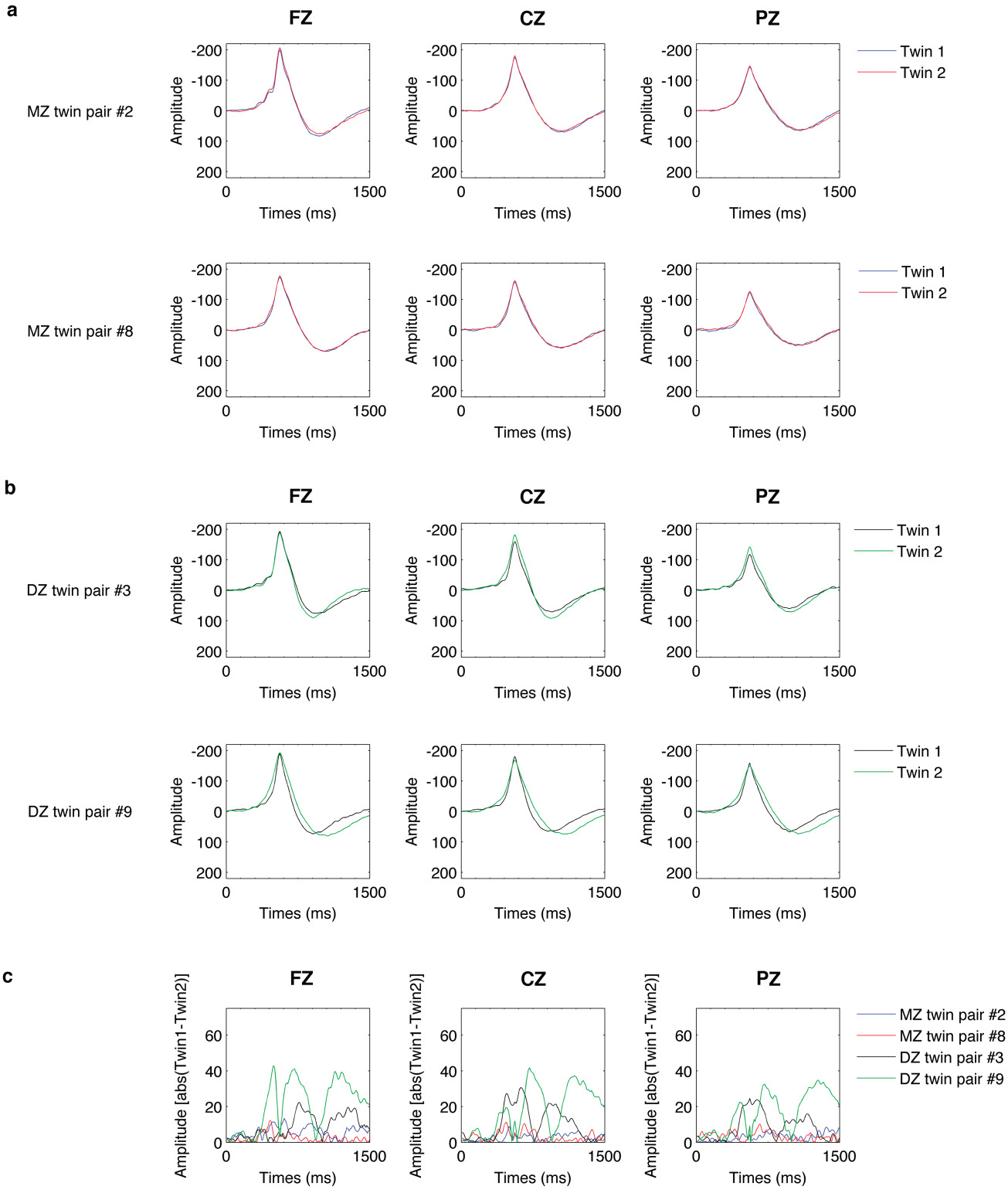

Figure 1. Individual KC average waveforms realigned to the negative peak in two representative MZ (a) and DZ (b) twin pairs at Fz (first column from the left), Cz (second column), and Pz (third column). Each line represents a twin pair. For each participant, the single KCs were time-locked to the large negative peak and then averaged considering the interval that goes from 550 ms before to 950 ms after the negative peak, obtaining an individual KC average waveform with a duration of 1500 ms and a negative peak at 550 ms. Data are plotted with upwards negative values on the y-axis. Amplitude is expressed in μV. Boxes in the fifth line (c) depict for each data point of the waveform the absolute value of the difference between twins belonging to the same representative MZ and DZ pair [abs(twin1 – twin2)].

Intraclass correlation coefficient

We used the intraclass correlation coefficient (ICC) to assess differences between within-twin pair resemblance in KC density, amplitude, and AUC. A bootstrapping analysis was performed to obtain levels of statistical significance for the observed ICCs [9, 17, 21]. Participant values were selected randomly with repetitions up to the same number as in the initial set with the aim to create a random distribution of the sample values, and then ICC was performed for each bootstrapped random sample (only positive ICC values were accepted). The bootstrap procedure was computed until 1000 positive ICC values were reached, obtaining a distribution of random ICCs. In line with previous studies [17, 21], for each considered variable, we present the original ICCs together with the upper percentile (p = 0.01) and median value of the bootstrapped data: ICC values above the bootstrap upper percentile value were considered statistically significant. ICC values are classically considered in slight agreement between 0 and 0.2, fair agreement between 0.21 and 0.40, moderate agreement between 0.41 and 0.60, substantial agreement between 0.61 and 0.80, and almost perfect agreement between 0.81 and 1 [59].

Cluster analysis

To further assess the within-pair similarity of the KC morphological pattern, we performed a hierarchical cluster analysis using PDIST and LINKAGE functions in MATlab on the KC average waveform profile, namely, the voltage values of all data points (the considered 1500 ms period) of the individual KC average waveform. Each individual KC average waveform profile was represented in 192 feature vectors, corresponding to the number of samples in the given time range (1500 ms with a sampling rate of 128 Hz). Vectors were grouped into a hierarchical cluster tree according to their proximity (Cityblock metric, shortest distance method). To depict the cluster trees, we used dendrograms composed by inverted U-shaped lines: the distance between elements was represented by the height of the U.

Results

Preliminary analyses

On a descriptive level, in both MZ and DZ groups, the KCs show higher mean density, amplitude, and AUC in the frontal region, with a progressive decrease along the midline for all the variables (Table 1).

The criterion for GVA of normal distribution was not fulfilled for density at Fz and Cz and for amplitude at Pz, so such variables were log-transformed in these specific derivations prior to all analyses. The results of the t-tests performed on KC variables to compare MZ and DZ are reported in Table 1, showing the absence of significant differences between the twin groups. No significant effect of covariates (MANCOVA) has been observed.

GVA and ICC on density, amplitude, and AUC

Table 2 reports results of GVA and ICC performed on KC density, amplitude, and AUC. ICCs for each variable and derivation are also graphically represented in Figure 2, a–c. GVA showed a significant genetic influence on amplitude variance at Pz and on AUC variance at Cz and Pz. ICC results showed that in MZ twins within-pair similarity was above the bootstrapping-based significance threshold (p = 0.01) at Cz and Pz for all variables, whereas only amplitude and AUC were above the significant threshold at Fz. Considering the classic ICC ranges [59], in MZ twins, within-pair similarity was almost perfect for AUC and amplitude at Cz and Pz and density at Pz, substantial for the other variables. In DZ twins, within-pair similarity was always below the significant threshold with the exception of density

Table 1. Means and SE of the KC parameters at Fz, Cz, and Pz for MZ and DZ twins

	Raw values			
Variables	MZ Mean (SE)	DZ Mean (SE)	t	P
KC Density Fz	1.71 (0.12)	1.55 (0.14)	0.93*	0.36
KC Density Cz	1.42 (0.12)	1.32 (0.13)	0.59*	0.56
KC Density Pz	0.87 (0.10)	0.84 (0.09)	0.17	0.90
KC Amplitude Fz	293.96 (5.62)	292.92 (5.46)	0.13	0.90
KC Amplitude Cz	260.47 (9.59)	263.70 (6.70)	−0.28	0.78
KC Amplitude Pz	216.03 (8.42)	220.19 (7.51)	−0.44*	0.66
KC AUC Fz	8335.20 (180.40)	8492.32 (251.87)	−0.51	0.61
KC AUC Cz	7184.28 (352.08)	7500.35 (244.00)	−0.74	0.46
KC AUC Pz	6189.11 (312.91)	6477.86 (237.47)	−0.73	0.48

The results of the MZ vs. DZ t-tests (t and p values) are also reported. When the criterion of normal distribution was not fulfilled, raw values were log-transformed.
*Indicates t-tests performed on log-transformed values.

Table 2. Genetic variance analysis and ICCs performed on KC parameters at Fz, Cz, and Pz

Variable	P	Analysis	ICC MZ	ICC DZ
KC Density Fz*	0.35	GWT	0.73 (0.77, 0.20)	0.67 (0.67, 0.19)
KC Density Cz*	0.5	GWT	0.72 (0.68, 0.20)	0.66 (0.66, 0.19)
KC Density Pz	0.28	GWT	0.83 (0.70, 0.20)	0.73 (0.70, 0.20)
KC Amplitude Fz	0.25	GWT	0.77 (0.69, 0.21)	0.63 (0.65, 0.19)
KC Amplitude Cz	0.06	GCT	0.95 (0.70, 0.21)	0.53 (0.63, 0.19)
KC Amplitude Pz*	**0.02**	GWT	0.92 (0.68, 0.17)	0.61 (0.66, 0.19)
KC AUC Fz	0.25	GCT	0.70 (0.68, 0.19)	0.09 (0.66, 0.19)
KC AUC Cz	**0.02**	GCT	0.96 (0.70, 0.21)	0.16 (0.69, 0.18)
KC AUC Pz	**0.03**	GCT	0.94 (0.72, 0.20)	0.19 (0.71, 0.19)

Results of genetic variance analysis (p-values); type of genetic variance estimate applied (GCT: combined among- and within-twin pair component estimate, GWT: within-pair estimate); ICCs for monozygotic (MZ) and dizygotic (DZ) twins reporting: original sample ICC (upper percentile of bootstrapped data, median of bootstrapped data). Results of the genetic variance analysis were significant for $p < 0.05$ (indicated in bold). For the ICCs, original sample ICC values above the bootstrap upper percentile value were considered statistically significant. *Analyses performed on log-transformed values.

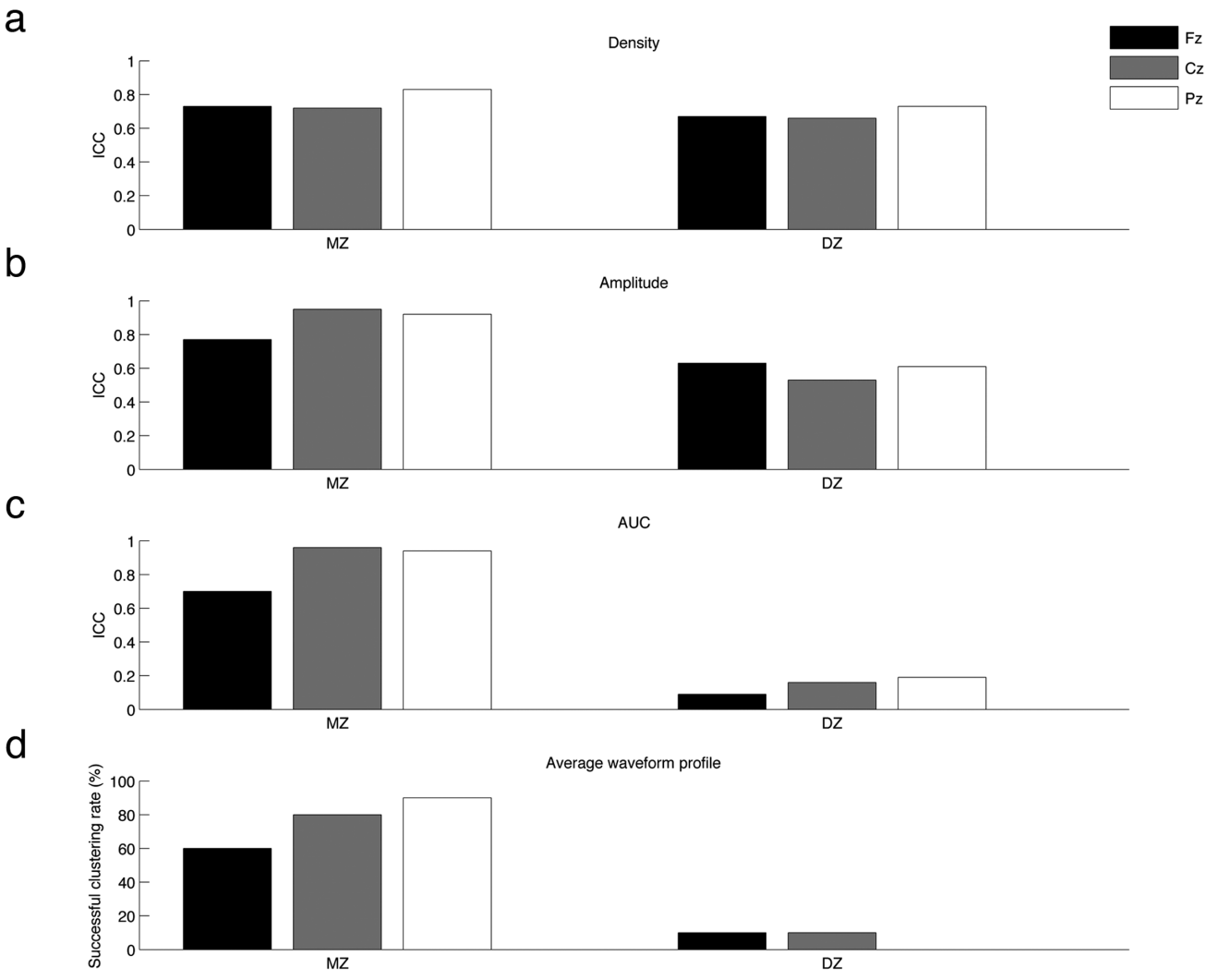

Figure 2. ICCs performed on KC density (a), amplitude (b), AUC (c), and percentage of successful clustering performed on the average waveform profile (d) at Fz (black bars), Cz (gray bars), and Pz (white bars) in MZ and DZ twin pairs.

at Pz. Moreover, within-pair similarity for AUC at Fz and Cz was below the bootstrapped median value, resulting lower than expected by chance. Considering the classic ICC ranges [59], in DZ twins within-pair similarity was substantial for density in all the derivations and amplitude at Fz and Pz, moderate for amplitude at Cz, slight for AUC in all the derivations.

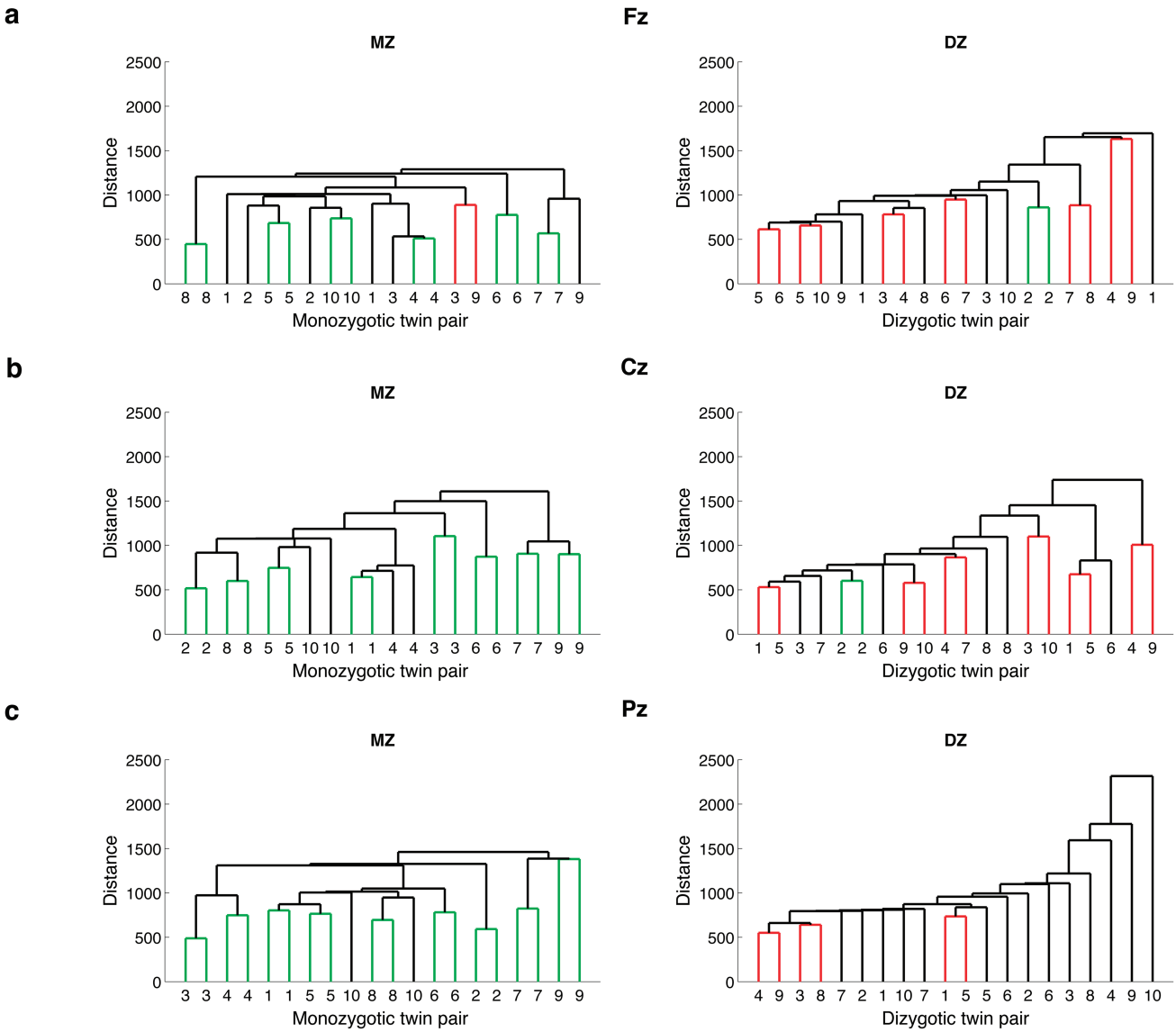

Figure 3. Dendrograms of cluster analysis based on the distance between individual KC average waveforms in MZ (left column) and DZ (right column) pairs at Fz (a), Cz (b), and Pz (c). On the x-axis, participants with the same number represent the same twin pair. Each dendrogram consists of several U-shaped black lines that connect objects in a hierarchical tree. Green U-shaped lines represent MZ or DZ pairs that clustered together and red U-shaped lines depict unrelated participants that cluster together.

Cluster analysis on KC average waveforms

Figure 3 shows the dendrograms of cluster analysis performed on the KC average waveforms at Fz, Cz, and Pz. The percentages of successful clustering for both groups in each derivation are depicted in Figure 2d. Results in the MZ group show that 6 of 10 twin pairs clustered at Fz, 8 of 10 clustered at Cz, and 9 of 10 clustered at Pz. On the contrary, in the DZ group, we found that only 1 of 10 twin pairs clustered at Fz and Cz, and none at Pz.

Discussion

In the present study, we compared for the first time several parameters of the spontaneous sleep KCs in MZ and DZ twin pairs, estimating the genetic effects (GVA) and the within-pair similarity (ICCs and cluster analysis). The ICCs showed marked differences in the within-pair similarity between MZ and DZ twins: density, amplitude, and AUC were significantly similar in the MZ groups with the remarkable exception of the density in the frontal area, whereas DZ twins always exhibited a within-pair similarity below the bootstrap-determined significant threshold with the exception of density at Pz. KC density showed the highest similarity between MZ and DZ pairs, whereas the greatest differences were observed for AUC at Cz and Pz, where within-pair similarity was almost perfect in MZ pairs and slight in DZ pairs. Consistently, we observed a significant genetic effect only on the AUC of the KC average waveform at the central and parietal (but not frontal) locations and on amplitude at Pz. Finally, in the MZ group, twin pairs accurately clustered for the KC average waveform with a higher frequency (successful clustering rate for MZ pairs: Fz = 60%; Cz = 80%; Pz = 90%) compared with DZ pairs (successful clustering rate for DZ pairs: Fz = 10%; Cz = 10%; Pz = none).

Taken together, these findings suggest a genetic control on the human KC. In particular, the morphological parameters of the KC (represented by the AUC and the profile of the KC average waveform) and the peak-to-peak amplitude, more than the KC density, exhibited the most solid evidence of a genetic component.

Our analyses extend the evidence of the heritability of the NREM sleep EEG. Indeed, a genetic effect has been observed for NREM sleep spectral composition [15, 16] and NREM sleep spindles [21], a NREM electrophysiological marker together with KC. More specifically, our results are consistent with the observation of a genetic effect in the δ band [16, 19], which is the frequency range that includes KCs.

Interestingly, the genetic effect seems to be smallest in the location where the KCs are maximally expressed: the frontal cortex. At a frontal level, no significant GVA has been observed, ICC in MZ was not significant for density (and only slightly above the significance threshold for AUC and amplitude), and the cluster analysis on KC average waveform showed a reduced successful clustering rate compared with central and parietal derivations. Consistently with our results, a recent study aimed at assessing the heritability of sleep oscillations in adolescent twins across brain regions found that slow oscillations (0.6–1.2 Hz) and slow-wave activity (1.4–4.6 Hz) were under a strong genetic control over the posterior areas, whereas unique environmental factors accounted for variance in slow oscillations (and to a lesser extent slow-wave activity) in the frontal regions [19]. Some features of the frontal KC regulation may have influenced these results. It should be considered that the KC represents an isolated cortical down-state [22]. Cortical down-states during sleep seem to be related to a decrease in synaptic strength that, homeostatically counterbalancing the wake-related synaptic strengthening, should promote sleep-dependent memory processes [60]. KCs, then, may be characterized by a homeostatic regulation process in relation with previous wakefulness, by which the frontal region is maximally affected. Indeed, sleep slow waves (including KCs) are characterized by both reactive and homeostatic features, and it has been recently proposed that these two modalities are parts of a double (instant/long-term) dynamic homeostatic regulation that protects the frontal region (and then cognitive functions) during sleep [61]. KCs undergo some of the homeostatic rules that characterize slow waves [37, 62], and the frontal areas exhibit the maximal expression of the slow-wave homeostatic regulation [63, 64]. These findings may indicate a stronger influence of environmental variables (e.g. environmental stimulation during previous wakefulness) on the frontal KCs compared with the central and parietal ones, which leads to a higher wake-dependent variability and, as a consequence, less uniform results about the genetic control in this area. It is worth noting that a recent study with intracranial stereo-EEG recordings found a large heterogeneity in KCs location and propagation [65]. According to the authors, such heterogeneity may be due to a variable involvement of cortico-thalamic and cortico-cortical networks in KCs generation and spread, and/or to the differential activation of several cortical regions during the previous waking period [65].

It has been also found that alcoholism has a negative impact on KC incidence and amplitude, and this effect is higher in the frontal region [66]. Moreover, we recently observed that the frontal area is the cortical region most affected by the reduction of KC density associated with AD [45]. Together, these findings suggest that the KCs in the frontal region may be more vulnerable than those in other cortical areas to potential sources of variability (e.g. processes related to pathological conditions and environmental influences), thus reducing the possibility to observe a genetic influence on KCs in this area, but this speculation needs to be directly assessed.

Another explanatory hypothesis is that the prevalent centro-parietal topography of the genetic influence observed in the present study is due to a higher contribution of the late positivity around 900 ms than the frontal negativity of the KC. It is worth noting that in sleep research the KC is often identified as the large negative peak around 550 ms, and the subsequent positivity is more difficult to detect, weaker, characterized by a higher variability [67], and often affected by the presence of other superimposed oscillations like sleep spindles [29]. Although the topography and the morphology of the negative peak have been widely studied and its frontal predominance is well-established [28], the local features of the following positive peak have received less attention. Albeit several studies on evoked KCs suggest a similar topography for the large negativity and the following positivity [27, 68], the possibility of a reduced "frontality" of the positive component compared with the negative one, at a speculative level, should be considered. The sources of the negative and positive components are not necessarily the same. Combining EEG and fMRI, KC-associated positive blood oxygen level dependent (BOLD) signal changes have been found in several subcortical (brainstem and thalamus), and cortical areas, mainly paracentral, posterior and inferior parieto-occipital, superior temporal, midline cingulate, and paracingulate regions [32, 69]. Albeit the temporal resolution of fMRI does not consent to identify the neural activity associated with the specific KC components, it has been proposed that the subcortical and cingulate BOLD changes may be associated with the production of the negative component of the KC, whereas BOLD changes in posterior and inferior cortical areas may be associated with the subsequent positivity [70]. Then, we cannot exclude that the reduced evidence for a genetic control on KC features in the frontal area reflects a higher genetic influence on the late positivity of the KC than on the classical frontal negativity. On the other hand, instead of a higher heritability of the positive component, the observed topography may represent a direct consequence of two methodological choices that can decrease the impact of the frontal negativity on our results: the assessment of KC amplitude with a peak-to-peak measure and the alignment to the negative peak for the assessment of the morphology of the average KC. The use of a peak-to-peak measure may have limited the possibility to observe a genetic effect at the frontal level, since the contribution of the frontal negativity could have been weakened by that of the later positivity. As far as the morphology of the average KC is concerned, the choice to time-lock the KCs to the negative peak may imply a reduction of the between-participants differences in correspondence with the negative component. Therefore, the observed genetic effect on the morphology of the KC should be mainly attributed to the positive component with a smaller impact of the frontal negativity, and this may be reflected by the prevalent centro-posterior topography of our results. In this view, our findings do not necessarily represent a higher heritability of the late positive component of the KC, whereas it could be a byproduct of the alignment to the negative peak. Since we have not performed separate analyses on the single components as viable studying

evoked KCs, we cannot provide a definitive conclusion about the nature of the observed topography of the KC heritability. Future studies should be directly aimed to disentangle this issue.

Although KC density and amplitude are variables usually investigated in KC studies, the KC area is often ignored. Our observation of a stronger genetic effect on KC AUC than on other parameters underlines a potential relevance of its assessment when studying changes in spontaneous and evoked KCs in normal, altered, and pathological conditions.

An important limitation of the present study is represented by the low sample size. The ICC values can be strongly affected by a great difference in a single twin pair when considering a small sample size, and this could explain the fact that DZ within-pair similarity for AUC was below the bootstrapping median value, which has scarce biological sense, as observed for some spindles parameters [21]. Our results, then, need to be replicated with a higher number of twin pairs. Another limitation is the absence of information about the cohabitation of the members of the same pair, so we cannot exclude the possible influence of this variable on our results. Finally, the alignment of the KCs to the large negative peak to obtain the individual KC average waveform may be considered a further limitation: the large amplitude of the negative component is partially a byproduct of such procedure, and this may have biased our results on the morphological aspects of the KCs. However, since this method has been used for both MZ and DZ pairs, it should have influenced both twin groups in a similar manner, with a minimal impact, then, on the assessment of the heritability of the KC.

In conclusion, our findings suggest the existence of a genetic component affecting the human KC, particularly influencing its morphology and amplitude, maximally expressed in central and parietal areas compared with the frontal one. If future studies will confirm our findings, extending them to larger samples, the morphology of the KC may represent a promising sleep-related endophenotype for future research on pathological conditions. Indeed, given the observed changes of KCs in AD [45, 55], our results further emphasize the possible role of the KC alterations as a biomarker for cognitive deterioration, recommending the importance of the investigation of the KC morphology in normal and pathological aging.

Conflict of interest statement. The authors declare that the research was conducted in the absence of any commercial or financial relationships that could be construed as a potential conflict of interest.

References

1. Feinberg I, *et al*. Period and amplitude analysis of NREM EEG in sleep: repeatability of results in young adults. *Electroencephalogr Clin Neurophysiol*. 1980;**48**(2):212–221.
2. Tan X, *et al*. High internight reliability of computer-measured NREM delta, sigma, and beta: biological implications. *Biol Psychiatry*. 2000;**48**(10):1010–1019.
3. Tan X, *et al*. Internight reliability and benchmark values for computer analyses of non-rapid eye movement (NREM) and REM EEG in normal young adult and elderly subjects. *Clin Neurophysiol*. 2001;**112**(8):1540–1552.
4. Finelli LA, *et al*. Individual 'fingerprints' in human sleep EEG topography. *Neuropsychopharmacology*. 2001;**25** (5 Suppl):S57–S62.
5. Buckelmüller J, *et al*. Trait-like individual differences in the human sleep electroencephalogram. *Neuroscience*. 2006;**138**(1):351–356.
6. De Gennaro L, *et al*. An electroencephalographic fingerprint of human sleep. *Neuroimage*. 2005;**26**(1):114–122.
7. Tucker AM, *et al*. Trait interindividual differences in the sleep physiology of healthy young adults. *J Sleep Res*. 2007;**16**(2):170–180.
8. Tarokh L, *et al*. The spectrum of the non-rapid eye movement sleep electroencephalogram following total sleep deprivation is trait-like. *J Sleep Res*. 2015;**24**(4):360–363.
9. Tarokh L, *et al*. Trait-like characteristics of the sleep EEG across adolescent development. *J Neurosci*. 2011;**31**(17):6371–6378.
10. Geyer H. Ueber den Schlaf von Zwillingen. *Z Indukt Abstamm Verebungsl*. 1937;**78**:524–527.
11. Zung WW, *et al*. Sleep and dream patterns in twins. Markov analysis of a genetic trait. *Recent Adv Biol Psychiatry*. 1966;**9**:119–130.
12. Linkowski P, *et al*. EEG sleep patterns in man: a twin study. *Electroencephalogr Clin Neurophysiol*. 1989;**73**(4):279–284.
13. Linkowski P, *et al*. Genetic determinants of EEG sleep: a study in twins living apart. *Electroencephalogr Clin Neurophysiol*. 1991;**79**(2):114–118.
14. Webb WB, *et al*. Relationships in sleep characteristics of identical and fraternal twins. *Arch Gen Psychiatry*. 1983;**40**(10):1093–1095.
15. De Gennaro L, *et al*. The electroencephalographic fingerprint of sleep is genetically determined: a twin study. *Ann Neurol*. 2008;**64**(4):455–460.
16. Ambrosius U, *et al*. Heritability of sleep electroencephalogram. *Biol Psychiatry*. 2008;**64**(4):344–348.
17. Adamczyk M, *et al*. Genetics of rapid eye movement sleep in humans. *Transl Psychiatry*. 2015;**5**:e598.
18. Markovic A, *et al*. Heritability of sleep EEG topography in adolescence: results from a longitudinal twin study. *Sci Rep*. 2018;**8**(1):7334.
19. Rusterholz T, *et al*. Nature and nurture: brain region-specific inheritance of sleep neurophysiology in adolescence. *J Neurosci*. 2018;**38**(43):9275–9285.
20. De Gennaro L, *et al*. Sleep spindles: an overview. *Sleep Med Rev*. 2003;**7**(5):423–440.
21. Adamczyk M, *et al*. Automatic sleep spindle detection and genetic influence estimation using continuous wavelet transform. *Front Hum Neurosci*. 2015;**9**:624.
22. Cash SS, *et al*. The human K-complex represents an isolated cortical down-state. *Science*. 2009;**324**(5930):1084–1087.
23. Contreras D, *et al*. Cellular basis of EEG slow rhythms: a study of dynamic corticothalamic relationships. *J Neurosci*. 1995;**15**(1 Pt 2):604–622.
24. Amzica F, *et al*. The K-complex: its slow (<1-Hz) rhythmicity and relation to delta waves. *Neurology*. 1997;**49**(4):952–959.
25. Amzica F, *et al*. The functional significance of K-complexes. *Sleep Med Rev*. 2002;**6**(2):139–149.
26. Davis H, *et al*. Electrical reactions of the human brain to auditory stimulation during sleep. *J Neurophysiol*. 1939;**2**:500–514.
27. Cote KA, *et al*. Scalp topography of the auditory evoked K-complex in stage 2 and slow wave sleep. *J Sleep Res*. 1999;**8**(4):263–272.

28. Colrain IM. The K-complex: a 7-decade history. *Sleep*. 2005;**28**(2):255–273.
29. Halász P. K-complex, a reactive EEG graphoelement of NREM sleep: an old chap in a new garment. *Sleep Med Rev*. 2005;**9**(5):391–412.
30. Amzica F, *et al*. Electrophysiological correlates of sleep delta waves. *Electroencephalogr Clin Neurophysiol*. 1998;**107**(2):69–83.
31. Wennberg R. Intracranial cortical localization of the human K-complex. *Clin Neurophysiol*. 2010;**121**(8):1176–1186.
32. Jahnke K, *et al*. To wake or not to wake? The two-sided nature of the human K-complex. *Neuroimage*. 2012;**59**(2):1631–1638.
33. Ehrhart J, *et al*. K-complexes and sleep spindles before transient activation during sleep. *Sleep*. 1981;**4**(4):400–407.
34. Niiyama Y, *et al*. Electrophysiological evidence suggesting that sensory stimuli of unknown origin induce spontaneous K-complexes. *Electroencephalogr Clin Neurophysiol*. 1996;**98**(5):394–400.
35. Bastuji H, *et al*. Evoked potentials as a tool for the investigation of human sleep. *Sleep Med Rev*. 1999;**3**(1):23–45.
36. Bastien CH, *et al*. EEG characteristics prior to and following the evoked K-Complex. *Can J Exp Psychol*. 2000;**54**(4):255–265.
37. Nicholas CL, *et al*. Increased production of evoked and spontaneous K-complexes following a night of fragmented sleep. *Sleep*. 2002;**25**(8):882–887.
38. Wauquier A, *et al*. K-complexes: are they signs of arousal or sleep protective? *J Sleep Res*. 1995;**4**(3):138–143.
39. De Gennaro L, *et al*. Topographical distribution of spindles: variations between and within nrem sleep cycles. *Sleep Res Online*. 2000;**3**(4):155–160.
40. Curcio G, *et al*. Effect of total sleep deprivation on the landmarks of stage 2 sleep. *Clin Neurophysiol*. 2003;**114**(12):2279–2285.
41. Halász P. The microstructure of sleep. *Suppl Clin Neurophysiol*. 2004;**57**:521–533.
42. Halász P, *et al*. The nature of arousal in sleep. *J Sleep Res*. 2004;**13**(1):1–23.
43. Terzano MG, *et al*. Origin and significance of the cyclic alternating pattern (CAP). Review article. *Sleep Med Rev*. 2000;**4**(1):101–123.
44. Terzano MG, *et al*. CAP and arousals are involved in the homeostatic and ultradian sleep processes. *J Sleep Res*. 2005;**14**(4):359–368.
45. De Gennaro L, *et al*. The fall of sleep K-complex in Alzheimer disease. *Sci Rep*. 2017;**7**:39688.
46. Crowley K, *et al*. An examination of evoked K-complex amplitude and frequency of occurrence in the elderly. *J Sleep Res*. 2002;**11**(2):129–140.
47. Kubicki S, *et al*. The effect of age on sleep spindle and K complex density. *EEG EMG Z Elektroenzephalogr Elektromyogr Verwandte Geb*. 1989;**20**(1):59–63.
48. Colrain IM, *et al*. Sleep evoked delta frequency responses show a linear decline in amplitude across the adult lifespan. *Neurobiol Aging*. 2010;**31**(5):874–883.
49. Crowley K, *et al*. The effects of normal aging on sleep spindle and K-complex production. *Clin Neurophysiol*. 2002;**113**(10):1615–1622.
50. Crowley K, *et al*. Evoked K-complex generation: the impact of sleep spindles and age. *Clin Neurophysiol*. 2004;**115**(2):471–476.
51. Prinz PN, *et al*. Changes in the sleep and waking EEGs of nondemented and demented elderly subjects. *J Am Geriatr Soc*. 1982;**30**(2):86–93.
52. Reynolds CF III, *et al*. EEG sleep in elderly depressed, demented, and healthy subjects. *Biol Psychiatry*. 1985;**20**(4):431–442.
53. Montplaisir J, *et al*. Sleep in Alzheimer's disease: further considerations on the role of brainstem and forebrain cholinergic populations in sleep-wake mechanisms. *Sleep*. 1995;**18**(3):145–148.
54. Crowley K, *et al*. Differentiating pathologic delta from healthy physiologic delta in patients with Alzheimer disease. *Sleep*. 2005;**28**(7):865–870.
55. Reda F, *et al*. In search of sleep biomarkers of Alzheimer's disease: K-complexes do not discriminate between patients with mild cognitive impairment and healthy controls. *Brain Sci*. 2017;**7**(5):E51.
56. Bastien CH, *et al*. Spontaneous K-complexes in chronic psychophysiological insomnia. *J Psychosom Res*. 2009;**67**(2):117–125.
57. Christian JC, *et al*. Choice of an estimate of genetic variance from twin data. *Am J Hum Genet*. 1974;**26**(2):154–161.
58. Christian JC, *et al*. Plasma cholesterol variation in the National Heart, Lung and Blood Institute Twin Study. *Genet Epidemiol*. 1987;**4**(6):433–446.
59. Landis JR, *et al*. The measurement of observer agreement for categorical data. *Biometrics*. 1977;**33**(1):159–174.
60. Tononi G, *et al*. Sleep function and synaptic homeostasis. *Sleep Med Rev*. 2006;**10**(1):49–62.
61. Halász P, *et al*. Two features of sleep slow waves: homeostatic and reactive aspects–from long term to instant sleep homeostasis. *Sleep Med*. 2014;**15**(10):1184–1195.
62. Rajna P, *et al*. Event-related non-specific responses (K-complexes) during sleep. *Acta Med Hung*. 1983;**40**(1):33–40.
63. Finelli LA, *et al*. Functional topography of the human nonREM sleep electroencephalogram. *Eur J Neurosci*. 2001;**13**(12):2282–2290.
64. Cajochen C, *et al*. Frontal predominance of a relative increase in sleep delta and theta EEG activity after sleep loss in humans. *Sleep Res Online*. 1999;**2**(3):65–69.
65. Mak-McCully RA, *et al*. Distribution, amplitude, incidence, co-occurence and propagation of human K-complexes in focal transcortical recordings. *eNeuro*. 2015;**2**(4). doi:10.1523/ENEURO.0028-15.2015
66. Colrain IM, *et al*. The impact of alcoholism on sleep evoked Delta frequency responses. *Biol Psychiatry*. 2009;**66**(2):177–184.
67. Cash SS, *et al*. Response to comment on "The human K-complex represents an isolated cortical down-state". *Science*. 2010;**330**:35.
68. Laurino M, *et al*. Disentangling different functional roles of evoked K-complex components: mapping the sleeping brain while quenching sensory processing. *Neuroimage*. 2014;**86**:433–445.
69. Caporro M, *et al*. Functional MRI of sleep spindles and K-complexes. *Clin Neurophysiol*. 2012;**123**(2):303–309.
70. Wennberg R, *et al*. On noninvasive source imaging of the human K-complex. *Clin Neurophysiol*. 2013;**124**(5):941–955.